In search for "healthy" landing zones for coronary stent placement: are the largest intrasegmental lumens adequate?

Igor Kranjec[1], Matjaž Klemenc[2], Dinko Zavrl Dzananovic[1], Matjaz Bunc[1], Igor D. Gregoric[2], Biswajit Kar[2]

[1]Department of Cardiology, University Medical Center, Ljubljana, Slovenia; [2]Department of Advanced Cardiopulmonary Therapies and Transplantation, The University of Texas Health Science Center at Houston, Houston, TX, USA

Contributions: (I) Conception and design: I Kranjec, M Klemenc, ID Gregoric; (II) Administrative support: ID Gregoric, B Kar; (III) Provision of study materials or patients: I Kranjec, M Klemenc, M Bunc; (IV) Collection and assembly of data: I Kranjec, M Klemenc, D Zavrl Dzananovic, M Bunc; (V) Data analysis and interpretation: I Kranjec, M Klemenc, D Zavrl Dzananovic; (VI) Manuscript writing: All authors; (VII) Final approval of manuscript: All authors.

Correspondence to: Igor D. Gregoric, MD. Department of Advanced Cardiopulmonary Therapies and Transplantation, The University of Texas Health Science Center at Houston, 6400 Fannin, Suite 2350, Houston, TX 77030, USA. Email: Igor.D.Gregoric@uth.tmc.edu.

Background: Coronary lesions are supposed to be enclosed between proximal and distal reference segments (RSs), the sites with the largest lumens within the same vessel segment. Finding "healthy" landing zones has been fundamental for efficient stent implantation. Consequently, our study aimed to determine, using optical coherence tomography (OCT), to what degree RSs conform to this concept.

Methods: Sixty-seven patients with a mean age of 63.5 years underwent culprit lesion stenting due to acute myocardial infarction (MI) (Group 1) or stable angina (Group 2). OCT was performed with commercially available equipment; all evaluations were made at RSs and minimal lumens.

Results: Normal vessel wall was infrequent (~10%) at RSs. Acceptable external elastic 220°) occurred in 55% to 67% and in 28% to 31% of RSs, respectively. Tissue composition at RSs was similar in both study groups except for a greater accumulation of thin-cap fibroatheromas (TCFA) in acute MI (29% in Group 1 *vs.* 9% in Group 2, P=0.035). Flow deterioration after stenting was associated with TCFA clusters extending from culprit main bodies into proximal RSs (P=0.008).

Conclusions: Optimal landing zones for stent placement should frequently be searched for beyond the culprit lesion segments although utilizing the largest intrasegmental lumens does not seem to cause immediate harm. However, TCFA at the landings should definitely be avoided.

Keywords: Optical coherence tomography (OCT); coronary lesion borders; percutaneous coronary intervention (PCI); landing zone

Introduction

Background

From a pathologist's perspective, coronary atherosclerosis is a focal instead of a diffuse intimal disease (1). In this context, a coronary lesion is supposed to be enclosed between proximal and distal reference segments (RSs) that are the sites with the largest lumens within the same vessel segment, although not with the least plaque (2,3). When performing a percutaneous coronary intervention (PCI), the distance covered by stenting should correspond with the lesion extent. If the stent is not optimally placed (i.e., "normal to normal", there remains a substantial risk of serious post-procedural complications (4). In diffuse coronary artery disease (CAD), it is quite challenging to accurately determine lesion borders and, consequently,

landing zones for stent placement.

Rationale and knowledge gap

Angiography is a standard method for assessing coronary anatomy and guiding PCI. Nevertheless, evaluating the lesion extent, composition, and plaque burden (PB) seems to be inadequate. Intravascular imaging with ultrasound (IVUS) and optical coherence tomography (OCT) are alternatives for assessment, they have both superior resolution and are extensively used. IVUS can precisely assess vessel structure and PB; atherosclerosis, for example, was found even in angiographically normal RSs (5). OCT provides exceptional axis (10–15 µm) and lateral resolution (25–40 µm), and OCT images share impressive similarity with histology (6). Several studies suggested that optimal landing zones should contain RSs with PB not exceeding 40% to 50% (7,8). Despite its somewhat limited ability to determine the total PB, OCT allows the calculation of the plaque-free wall (PFW); indeed, a PFW angle ≥220° has been proposed as a surrogate indicator for the PB <40% (9).

Objective

In contrast to the main bodies of coronary lesions, a paucity of literature reviews the identification of lesion boundaries. The objective of our study was to characterize by OCT the borders of culprit lesions that conformed to the definition above (2,3). We sought to appraise the adequacy of RSs to provide suitable landing zones. Finally, we explored the impact of the selected zones on peri-procedural complication. This manuscript is written following the STROBE reporting checklist (available at https://jtd.

Highlight box

Key findings
- Current lesion definition is not consistent with healthy segmental reference sites.

What is known and what is new?
- Finding the landing zones with low plaque burden is essential for stent placement.
- Additional thin-cap fibroatheromas appear at infarct-related lesion borders.

What is the implication, and what should change now?
- We recommend using external elastic membrane instead of maximal lumens to find appropriate landings.

---

amegroups.com/article/view/10.21037/jtd-23-924/rc).

Methods

Study design and population

We conducted a retrospective study to investigate the borders of the culprit lesions in patients who underwent elective or urgent PCI at our institution from February 6, 2015, through October 9, 2020. Baseline and post-stenting OCT were mandatory for inclusion in the study. Identification of the culprits involved electrocardiography, non-invasive tests, and lesion morphology. Patients with Type 1 myocardial infarction (MI) (10) were assigned to Group 1, and those with stable angina were placed in Group 2. Individuals with MI in the same myocardial areas, previous PCI or surgical coronary revascularization of culprit arteries, non-obstructive or non-culprit lesions, missing initial or post-stenting pullbacks, or suboptimal OCT examinations were excluded (Figure S1). Clinical data were collected by reviewing medical records, and procedural details were entered into a database at the time of PCI. Two independent researchers comprehensively analyzed the OCT images; in case of disagreement, a consensus had to be reached. The study was conducted in accordance with the Declaration of Helsinki (as revised in 2013). The retrospective analysis was approved by the Institutional Review Board of General Hospital Dr. Franc Derganc, Ul. Padlih borcev 13A, 5290 Šempeter pri Gorici (SBG 4/2023). The individual consent was waived because of the retrospective manner of the analysis.

Diagnostic and therapeutic procedures

Invasive procedures were performed with standard radiographic equipment, technique, and catheters. Coronary angiography was completed in multiple projections, and the view showing the worst stenosis was used for further analysis. OCT was performed using a commercially available Fourier-domain OCT system (Ilumien Optis, Abbott Vascular, Santa Clara, CA, USA) and a 2.7-F imaging catheter (Dragonfly Duo/Optis, Abbott Vascular, Santa Clara, CA, USA). In occluded vessels, a predilatation with a small balloon (i.e., ≤2.0 mm) was allowed to enable the passage of the imaging probe. Automated pullback at the speed of 20 mm/s, assisted by a power contrast injector, was accomplished after nitroglycerin administration to examine the culprit vessel in a survey or high-resolution mode.

Baseline and post-stenting examinations were digitally stored for further analysis. PCI was performed according to contemporary practice. Antiplatelet and antithrombin drugs were given at the start of the procedure, and thrombo-aspiration was used in the case of a high thrombus burden. Six PCI operators were instructed to use the largest intra-segmental lumens as the landing zones, according to the practice at the time, and avoid extensive lipid-rich tissues. The technicians provided the required measurements, while the selection of the landing zones and stents was the operator's decision.

Angiographic analysis

Angiographic definitions are explained in the Appendix 1. Quantitative analysis with an edge detection system was used to compute percent diameter stenosis (%DS). Lesion length was measured as a distance between seemingly normal proximal and distal sites. The lesions were graded as discreet (<10 mm), tubular (10–20 mm), and diffuse (>20 mm) (11). They were located in 15 segments according to the American Heart Association reporting system (12). The grades of blood flow were assessed by the Thrombolysis in Myocardial Infarction (TIMI) Grade Flow scoring system (13); grades ≤2 were considered to be impaired flow. Post-stenting edge dissections were categorized according to the National Heart, Lung, and Blood Institute classification system (14).

OCT analysis

OCT definitions are described in Appendix 1. Quantitative analysis of culprit lesions was performed at RSs and minimum lumens with proprietary software (Abbott Vascular, Santa Clara, CA, USA). Segments were screened in the lumen profile, and the OCT system automatically tracked lumen contours, located maximum and minimum lumens, and computed percent area stenosis (%AS). The length was measured as the distance from proximal to distal RSs [lumen-based approach (LBA)] or, from proximal to distal intra-segmental border sites showing sufficient external elastic membrane [EEM-based approach (EBA)]. Qualitative analysis was performed at RSs and adjacent marginal segments (AMSs) up to 5 mm beyond RSs (*Figure 1*). The analysis involved border visibility, presence and types of atherosclerotic plaques, and post-stenting edge dissections. Border visibility was acceptable if the EEM appeared in ≥180° of the vessel circumference; EEM in

≥220° indicated a PB <40% (9,15). Normal vessel wall was distinguished by a three-layered structure with a maximum thickness of ≤300 μm; a width up to 600 μm was considered a non-atherosclerotic adjustment (16). Plaques were classified as fibrous plaque (FP), fibrocalcific plaque (FCP), thick-cap fibroatheroma (ThCFA), thin-cap fibroatheroma (TCFA), and calcified nodules (3). TCFA were defined as a lipid-rich plaque with a fibrous cap thickness of <65 μm and a maximum lipid arc >90° (2). The landing zones were optimal ("normal to normal") or acceptable (PFW angle ≥220° without extensive lipid-rich tissues) (7-9).

Edge dissections were defined as disruptions of the luminal vessel surface 5 mm beyond stent edges; they were further divided into major or minor dissections (6).

Endpoints

The OCT endpoint was a proportion of optimal ("normal to normal") and acceptable landing zones (PFW angle ≥220°) in the whole group, patients with acute MI, and those with stable angina. Similarly, the PCI endpoint was a proportion of periprocedural complications (i.e., TIMI blood flow ≤2, edge dissections) in the whole group, patients with acute MI, and those with stable angina.

Statistical analysis

Continuous variables were shown as means with standard deviations or medians with interquartile ranges when the distribution was not normal. Categorical variables were displayed as frequencies with percentages. A Student's t-test and χ^2 test or Fischer exact test were used to compare continuous and categorical variables, respectively. Logistic regression analysis was used to predict the risk of peri-procedural complications (TIMI flow grades ≤2 and stent edge dissections). All tests were two-tailed, and statistical significance was considered for P values <0.05. All analyses were performed using IBM SPSS software (version 20.0, SPSS Inc., Chicago, IL, USA).

Results

A total of 67/101 (66%) patients planned for single culprit lesion PCI with available OCT were enrolled in the study; 34 (34%) patients were excluded for various reasons (Figure S1). Thirty-four patients (Group 1) presented with acute MI, 11 with ST-segment elevation MI (STEMI), and 18 with non-ST-segment elevation MI. The remaining
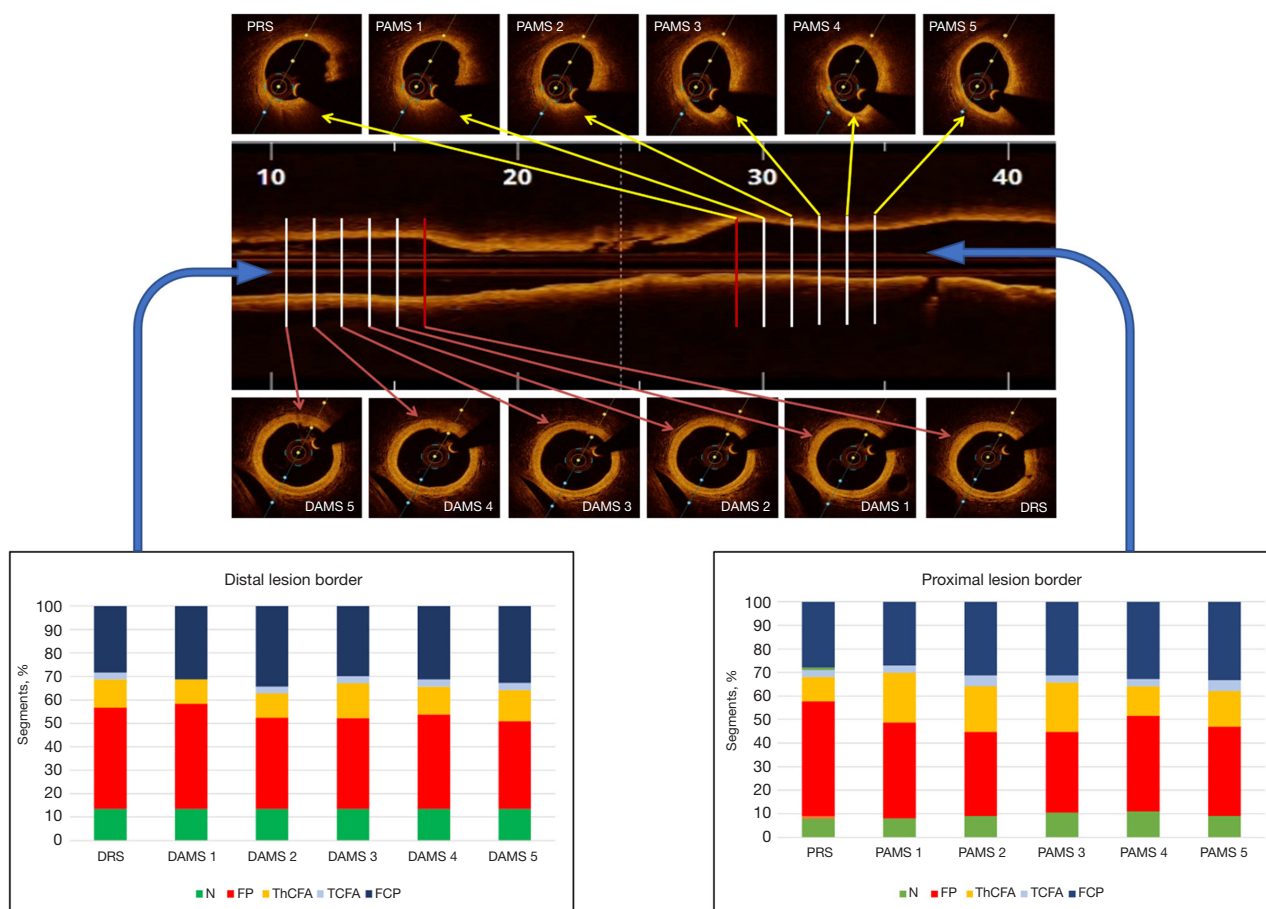
Figure 1 Analysis of the culprit lesion borders. Upper panel. The culprit lesion is enclosed between two red lines. Proximal and distal reference segments are the sites with the largest lumens within the same vessel segment. Adjacent marginal segments are examined at 1-mm intervals up to 5 mm beyond the reference segments. Lower panel. The composition of the vessel wall is shown at proximal (right) and distal lesion borders (left). The normal vessel structure (green bars) is quite infrequent on both sides of the border. The prevailing components are fibrous (red bars) and FCPs (dark blue bars). PRS, proximal reference segment; DRS, distal reference segment; PAMS 1–5, proximal adjacent marginal segments 1 to 5 mm beyond the proximal reference segment; DAMS 1–5, distal adjacent marginal segments 1 to 5 mm beyond the distal reference segment; N, normal vessel structure; FP, fibrous plaque; ThCFA, thick-cap fibroatheroma; TCFA, thin-cap fibroatheroma; FCP, fibrocalcific plaque.

33 patients (Group 2) had stable angina. Clinical characteristics are summarized in *Table 1*. Most patients were males in their mid-sixties, and nearly 20% had diabetes. Group 2 patients were older, expressed different risk factors, suffered from long-standing symptoms, and some were already taking antiplatelet drugs and statins.

Angiographic characteristics are shown in *Table 1*. For all patients, culprit lesions usually appeared in proximal segments, their median %DS was 90%, and only 9% of lesions were discreet. In Group 1, the culprits were narrower and more evenly distributed between epicardial

arteries.

Quantitative OCT characteristics are shown in *Table 2*. The lesions appeared in sizeable arteries with significant tapering (median cross-sectional area, proximally 7.63 mm^2 *vs.* distally 6.84 mm^2, P<0.001). Luminal dimensions at the borders were comparable in both study groups, while %AS was significantly greater in Group 1 (P=0.019). Lesion lengths were measured by two OCT methods that diverged significantly (median length, LBA 17 mm *vs.* EBA 19 mm, P<0.001); insufficient EEM visibility at RSs prevented EBA calculations in 16 (24%) patients. Importantly, LBA

Table 1 Clinical and angiographic characteristics

Variables	All patients (n=67)	Group 1 (n=34)	Group 2 (n=33)	P value
Age, years	63.5±11.3	60.3±12.6	66.8±8.9	0.018
Male	44 (65.7)	22 (64.7)	22 (66.7)	0.866
Hypertension	48 (71.6)	20 (58.8)	28 (84.8)	0.018
Hypercholest	28 (41.8)	13 (38.2)	15 (45.5)	0.549
Diabetes	12 (17.9)	5 (14.7)	7 (21.2)	0.487
Smoking	13 (19.4)	10 (29.4)	3 (9.1)	0.035
Prior AP	28 (41.8)	1 (2.9)	27 (81.8)	<0.001
Prior MI	11 (16.4)	0	11 (33.3)	<0.001
Prior PCI	17 (25.4)	1 (2.9)	16 (48.5)	<0.001
Prior aspirin	27 (40.3)	3 (8.8)	24 (72.7)	<0.001
Prior thyenopiridins	6 (9.0)	0	6 (18.2)	0.009
Prior statins	18 (26.9)	5 (14.7)	13 (39.4)	0.023
1–3 VD				
1-VD	46 (68.7)	23 (67.6)	23 (69.7)	0.856
2-VD	16 (23.9)	7 (20.6)	9 (27.3)	0.521
3-VD	5 (7.5)	4 (11.8)	1 (3.0)	0.174
Culprit				0.032
LCA	5 (7.5)	2 (5.9)	3 (9.1)	
LAD	35 (52.2)	14 (41.2)	21 (63.6	
LCX	13 (19.4)	6 (17.6)	7 (21.2)	
RCA	14 (20.9)	12 (35.3)	2 (6.1	
Segment				0.221
1	2 (3.0)	2 (5.9)	0	
2	10 (14.9)	9 (26.5)	1 (3.0)	
3	2 (3.0)	1 (2.9)	1 (3.0)	
5	5 (7.5)	2 (5.9)	3 (9.1)	
6	19 (28.4)	8 (23.5)	11 (33.3)	
7	15 (22.4)	5 (14.7)	10 (30.3)	
8	1 (1.5)	1 (2.9)	0	
11	7 (10.4)	3 (8.8)	4 (12.1)	
12	2 (3.0)	1 (2.9)	1 (3.0)	
13	4 (6.0)	2 (5.9)	2 (6.1)	
Proximal segment	60 (89.6)	31 (91.2)	29 (87.9)	0.659
%DS	90 [80–99]	97 [90–100]	80 [70–90]	<0.001

Table 1 (*continued*)

Table 1 (*continued*)

Variables	All patients (n=67)	Group 1 (n=34)	Group 2 (n=33)	P value
Occlusion	12 (17.9)	12 (35.3)	0	<0.001
Length				0.182
Discreet, <10 mm	6 (9.0)	1 (2.9)	5 (15.2)	
Tubular, 10–20 mm	39 (58.2)	20 (58.8)	19 (57.6)	
Diffuse, >20 mm	22 (32.8)	13 (38.2)	9 (27.3)	

Values are mean ± standard deviation, median [25th, 75th percentiles], or n (%), as appropriate. Groups 1 and 2 are compared using unpaired *t*-test for equality of means or χ^2 test. Group 1, patients with acute MI; Group 2, patients with stable AP. Hypercholest, hypercholesterolemia; AP, angina pectoris; MI, myocardial infarction; PCI, percutaneous coronary intervention; 1–3 VD, number of vessels with angiographically significant coronary artery stenosis; LCA, left coronary artery; LAD, left anterior descending coronary artery; LCX, left circumflex coronary artery; RCA, right coronary artery; %DS, percent diameter stenosis.

dimensions closely resembled angiographic measurements.

EEM visibility at the lesion borders is presented in Table S1. Acceptable visibility (EEM ≥180°) was confirmed in 67% of the proximal and 55% of the distal RSs; exploring distal, but not proximal AMSs, somewhat improved visibility. Acceptable PB (PFW angle ≥220°) was discovered in 28% of the proximal and 31% of the distal RSs; PB increased at proximal AMSs by 32% (P=0.023), while it decreased distally by 33% (P=0.005). There were no significant differences between the groups.

The vessel wall composition at the lesion borders is shown in Tables S2-S7 and *Figure 2*. The normal structure was surprisingly uncommon: it was discovered in 9% of the proximal and 13.5% of the distal RSs and remained infrequent at AMSs. Plaques prevailing at both borders were FP, followed by FCP and ThCFA. TCFA were found at minimal lumens in 24 (35.8%) patients and at lesion borders in 13 (19.4%) patients; they occurred in 7.6% of RSs and 16.4% of AMSs (*Table 2*). In Group 1, as compared with Group 2, TCFA accumulations were more frequent at minimum lumens (67.6% *vs*. 3.0%, P<0.001) as well as proximal borders (29.4% *vs*. 9.1%, P=0.035).

OCT discovered optimal landing zones in 9% of proximal and 13.5% of distal RSs. Acceptable landing zones appeared in 28% of proximal and 31% of distal RSs. No significant differences were seen between the study groups.

Table 2 Optical coherence tomography quantitative and qualitative characteristics

Variables	All patients (n=67)	Group 1 (n=34)	Group 2 (n=33)	P value
Quantitative OCT characteristics[†]				
Lesion diameter and area				
Prox D, mm	3.34 [3.05–3.79]	3.29 [3.04–3.75]	3.41 [3.10–3.87]	0.845
Min D, mm	1.68 [1.36–2.18]	1.55 [1.15–1.96]	1.83 [1.51–2.27]	0.215
Dist D, mm	3.13 [2.67–3.64]	3.20 [2.60–3.74]	3.1 [2.72–3.45]	0.408
Prox area, mm^2	7.63 [6.03–9.85]	7.47 [6.22–10.38]	7.83 [5.84–9.76]	0.410
Min area, mm^2	1.59 [1.15–2.74]	1.42 [0.86–1.95]	1.97 [1.36–3.06]	0.249
Dist area, mm^2	6.84 [5.38–8.54]	6.62 [4.26–9.03]	6.85 [5.63–8.25]	0.795
%AS	78 [69–86]	83 [76.30–89]	74 [65–84]	0.019
Lesion length				
Angio length, mm	17.5 [13.2–23.1]	19.8 [15.1–27.7]	16.5 [13.2–20.1]	0.013
LBA length, mm	17 [13–23]	18 [13–25]	17 [13.5–21]	0.676
EBA length[‡], mm	19 [15–26]	20 [16–28]	18.5 [14.3–23.5]	0.562
Qualitative characteristics[†]				
Thin-cap fibroatheromas at reference and adjacent marginal segments				
All TCFA	13 (19.4)	10 (29.4)	3 (9.1)	0.035
RS	5 (7.5)	5 (14.7)	0	0.022
Prox RS	3 (4.5)	3 (8.8)	0	0.081
Dist RS	2 (3.0)	2 (5.9)	0	0.157
AMS	11 (16.4)	8 (23.5)	3 (9.1)	0.111
Prox AMS	5 (7.5)	5 (14.7)	0	0.022
Dist AMS	7 (10.4)	4 (11.8)	3 (9.1)	0.721

Values are n (%) or median (25th, 75th percentiles), as appropriate. Groups 1 and 2 are compared using unpaired *t*-test for equality of means or χ² test. [†], the majority of qualitative characteristics are shown in Table S2. Group 1, patients with acute myocardial infarction; Group 2, patients with stable angina. Prox D, proximal reference diameter; Min D, minimal lesion diameter; Dist D, distal reference diameter; Prox Area, proximal reference area; Min Area, minimal lesion area; Dist Area, distal reference area; %AS, percent area stenosis; Angio length, distance between angiographically determined reference segments; LBA length, distance between reference segments determined by lumen-based approach; EBA length, distance between reference segments determined by external elastic membrane-based approach ([‡], data collected from 51 patients); TCFA, thin-cap fibroadenoma; RS, reference segments; Prox RS, proximal reference segments; Dist RS, distal reference segments; AMS, adjacent marginal segments; Prox AMS, proximal adjacent marginal segments; Dist AMS, distal adjacent marginal segments.

PCI characteristics are displayed in *Table 3*. Overall, the median stent diameter was 3.5 mm, and the cumulative length was 22.5 mm. The stents were larger and slightly longer in Group 1. At the end of PCI, TIMI flow ≤2 was detected in 5 (7.5%) enrolled patients, more frequent in Group 1 (14.7% *vs.* 0% in Group 2, P=0.029). OCT discovered more stent edge dissections than angiography (26.9% *vs.* 19.4%, respectively; P=0.024). Based on OCT,

the dissections were more frequent in Group 1 (38.2% *vs.* 15.2% in Group 2, P=0.039), and nearly half required additional stenting.

Finally, logistic regression analysis was used to predict peri-procedural complications (Table S8). Using univariate analysis, the risk of TIMI flow ≤2 following stenting diminished in patients without STEMI [odds ratio (ORs) =0.049, 95% confidence interval (CI): 0.005–0.49; P=0.010]
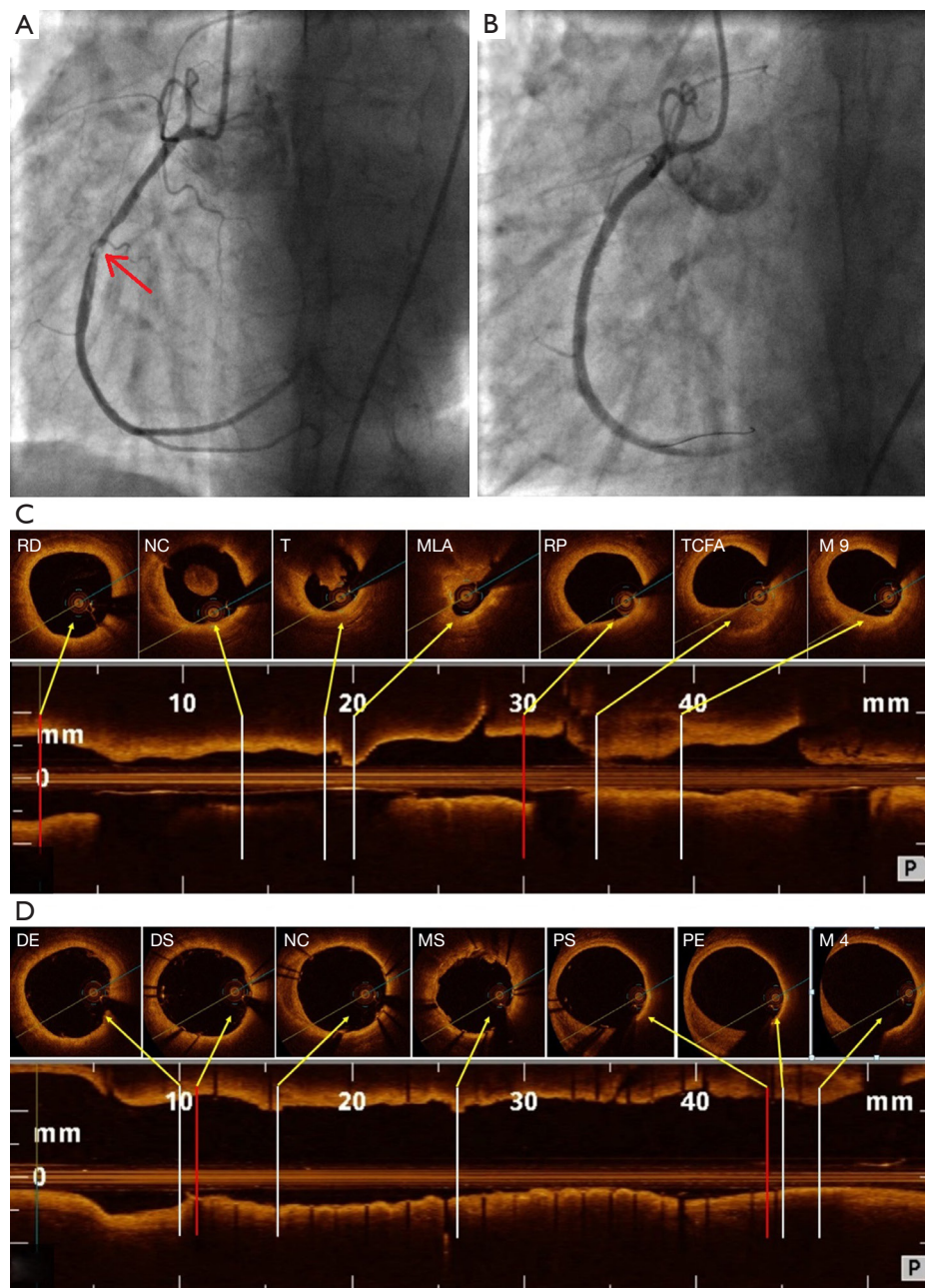
Figure 2 Complex pathogenetic mechanism resulting in blood flow deterioration after stent placement. (A) Initial angiography showed a thrombotic obstruction of the mid-right coronary artery (red arrow) with a preserved antegrade flow; (B) angiography after stent placement demonstrated a slow flow after direct implantation of two drug-eluting stents (3.0 mm ×15 mm each). (C) Initial OCT in a survey mode showed a 30-mm long lesion between two red lines. Inside the lesion, a ruptured plaque at MLA, long thrombus (T), and additional NC (at 9 o'clock) are seen. Please note a vulnerable plaque (TCFA, at 6 o'clock) 4 mm beyond the proximal lesion border. (D) OCT in a survey mode, performed after stent placement, showed two stents between the red lines. There is an almost complete disappearance of the thrombus at the MS, while the intra-lesion NC (at 9 o'clock) persisted. Please note that PS landed onto TCFA (at 7 o'clock). RD, reference distal; NC, necrotic core; T, thrombus; MLA, minimum lumen area; RP, reference proximal; TCFA, thin-cap fibroatheroma; M9, marginal segment 9 (i.e., 9 mm beyond RP); DE, distal edge; DS, distal stent struts; MS, mid-stent segment; PS, proximal stent struts; PE, proximal edge; M4, marginal segment 4 (i.e., 4 mm beyond PS); OCT, optical coherence tomography.

464

Kranjec et al. "Healthy" landing zones for coronary stent placement

Table 3 Percutaneous coronary intervention characteristics

Variables	All patients (n=67)	Group 1 (n=34)	Group 2 (n=33)	P value
Stents, n	1.2±0.7	1.3±0.7	1.0±0.6	0.065
Stent diam, mm	3.5 (3.0–3.5)	3.5 (3.0–3.9)	3.0 (3.0–3.5)	0.008
Cumul length, mm	22.5 (18.0–32.5)	24.5 (18.0–37.5)	20.0 (15.0–27.5)	0.166
TIMI flow 0–3	2.9±0.2	2.8±0.3	3.0±0.0	0.029
TIMI flow ≤2	5 (7.5)	5 (14.7)	0 (0)	0.029
Ang dissect	13 (19.4)	8 (23.5)	5 (15.2)	0.386
Ang dissect type				0.705
A	7 (10.4)	4 (11.8)	3 (9.1)	
B	5 (7.5)	3 (8.8)	2 (6.1)	
C	1 (1.5)	1 (2.9)	0 (0)	
OCT dissect	18 (26.9)	13 (38.2)	5 (15.2)	0.039
OCT dissect type				0.101
Major	8 (11.9)	6 (17.6)	2 (6.1)	
Minor	10 (14.9)	7 (20.6)	3 (9.1)	

Values are mean ± standard deviation, median (25th, 75th percentiles), or n (%), as appropriate. Groups 1 and 2 are compared using unpaired t-test for equality of means or χ^2 test. Group 1, patients with acute myocardial infarction; Group 2, patients with stable angina. Stent diam, stent diameter; Cumul length, cumulative stent length; TIMI, thrombolysis in myocardial infarction; Ang dissect, edge dissections detected by angiography; OCT dissect, edge dissections detected by optical coherence tomography.

or without TCFA at proximal RSs (OR =0.028, 95% CI: 0.002–0.4; P=0.008); however, multivariate analysis ascertained that only STEMI absence reduced the risk for impaired flow after stenting (OR =0.032, 95% CI: 0.002–0.825; P=0.037). As determined by univariate analysis, stent edge dissections were associated with several clinical factors and larger stent diameters (OR =3.98, 95% CI: 1.12–14.11; P=0.032); however, none of the listed variables were able to predict dissections by multivariate analysis.

Discussion

Key findings

Searching for "healthy" landing zones has been appreciated as one of the fundamental principles of efficient stent implantation (2). Our results indicated that (I) normal vessel wall enabling optimal stent placement was infrequent at the largest intra-segmental lumens delineating the culprit lesions; (II) PB at those sites exceeded recommended threshold in approximately 70% of study participants; (III) tissue composition at the culprit borders was similar in patients with stable angina and acute MI except for

increased clusters of TCFA in the latter group; (IV) RSs determined by the largest intra-segmental lumens underestimated true lesion lengths; (V) available variables allowed us to anticipate only post-procedural blood flow impairment.

Strengths and limitations

A balanced structure of the study population and detailed analysis of the data acquired by histology resembling OCT imaging were perceived to be the strength of our study. The proportional equipoise between patients with stable angina and acute MI was difficult to obtain; however, it enabled a comparison between two different pathologic conditions. Limitations of our study included those inherent to retrospective analysis and single-center studies. The sample size was small and lack statistical power to make inferences other than the generation of a hypothesis. The precise placement of the stents over the selected landing zones was not confirmed by the co-registration of angiography and OCT. Finally, the adequacy of our stent sizing/placing technique was tested only on peri-procedural complications.

Comparison with similar research

Complying with the classification proposed by Radu (16), we only detected the normal structure in 9% of the proximal and 13.5% of the distal RSs. In a similar IVUS study (5), the normal appearance occurred in 6.8% of the angiographically disease-free RSs. Unsurprisingly, we found atherosclerotic plaques in 91% of the proximal and 86% of the distal RSs. Similar results were published by Gonzalo and colleagues (17). Given the limited penetration depth of the near-infrared light used by OCT, the accurate assessment of PB is hardly realistic. However, a significant correlation between PB (assessed by IVUS) and PFW (determined by OCT) has been recently reported; PFW <220° indicated a suboptimal landing zone in 78% of cases, whereas PFW ≥220° prevented excessive stenting in 84% of cases (9). We detected PFW ≥220° in only 28% of the proximal and 31% of the distal RSs; PB increased in the proximal AMSs by 32% and decreased distally by 33%. It might be argued that the majority of intra-segmental RSs did not represent the optimal landing zones.

In contrast to the main body of the culprit lesions, there is a paucity of data on TCFA at their boundaries. A systematic examination of the coronary arteries with IVUS showed that TCFA are typically clustered at the proximal vessel segments (18). In patients with STEMI, stent placement failed to cover the whole lesion length in about 50% of all procedures, leaving behind stent edges necrotic cores and TCFA (19). In our study, TCFA were detected at RSs and related AMSs in approximately 20% of all patients, particularly in Group 1.

The LBA method is always available, while EBA requires at least 180° of the EEM to be visible. The Ilumien III trial (20) found sufficient EEM visibility in 84% of patients. Conversely, we recognized EEM ≥180° in 67% of the proximal and 55% of the distal RSs.

There is an unsettled balance between adequate lesion coverage and using excessively long stents. Diffuse coronary stenoses are associated with a 17% increased risk of major adverse cardiac events for every 10 mm of stent deployed (21). Angiography and LBA yield shorter stent lengths but are associated with an increased risk of geometric miss. If the 180° EEM visibility at the LBA-determined RSs had been applied, the lesion length could be measured in 76% of our cases. We suggest that the landing zones with a ≥220° EEM visibility (i.e., PFW angle ≥220°) should be pursued, even outside the target segments.

Previous studies linked the TCFA-containing lesions with a risk of distal embolization and Type IVa MI (22). Indeed, in our study, TCFA at proximal lesion borders extending beyond the culprit minimal lumens were associated with peri-procedural blood flow impairment (*Figure 2*). However, according to multivariate analysis and data in the literature (23), a complex pathogenetic mechanism generating flow deterioration has been suggested. The incidence of stent edge dissections depends on the diagnostic method used: it was reported to be 1.7% to 4.8% for angiography, 7.8% to 20% for IVUS, and 15.5% to 23.6% for OCT (24). The risk of dissection is six times higher when the stent is placed over a diseased region abundant with FCP, lipid-rich plaques, and TCFA (18). The frequency of dissections in our study was comparable to other results; however, despite the higher rates in the acute MI group, we did not show any association with the plaque composition at the lesion borders.

Explanation of findings

The normal vessel wall is a three-layered structure composed of the intima, media, and adventitia with a thickness <250 µm (25). An excellent agreement in measuring the intima was reported between histology and OCT (26). In the latter, a cut-off of 300 µm was applied to differentiate between the normal intima and adaptive changes and >600 µm to identify the pathological intimal thickness that denotes the end of the "healthy" vessel wall (16).

The distance to be covered by stenting should correspond with the lesion extent; otherwise, there remains a substantial risk of post-procedural MI, restenosis, and stent thrombosis (4). Many pathologists perceive atherosclerosis as a focal disease (1); however, the accumulated evidence does not comply with this limited view. First, accurate lesion borders are difficult to establish with angiography as the plaques are invisible until the lesion occupies 40% to 50% of the vessel cross-section (8). Furthermore, when atherosclerosis appears at any vessel site, it is almost impossible to find a normal segment (5). In patients with advanced CAD, diffuse "plaquing" was revealed in 90% of the arteries (27). Finally, invasive measurements of coronary blood flow allowed the pattern of CAD to be characterized as focal, diffuse, or mixed distribution (28).

TCFA are considered precursors of plaque rupture and, consequently, unstable clinical presentations. They are defined as lesions with fibrous caps <65 µm, large lipid cores, and macrophage infiltration (29). Currently, OCT is the only imaging modality with sufficient resolution to

466

Kranjec et al. "Healthy" landing zones for coronary stent placement

identify TCFA. In their seminal study, Jang *et al.* found TCFA in 72% of the acute MI patients and only 20% of their stable counterparts (30).

The important role of OCT imaging is to recognize the culprit lesions, assess their morphology, find suitable landing zones, and enable accurate stent sizing/placing. A healthy vessel wall is certainly the best landing zone, though a moderate amount of PB seems acceptable (6). PCI can be associated with a small but not negligible incidence of peri-procedural complications. For example, blood flow deterioration was reported in 0.6% to 5% of elective PCI and 12% to 32% of primary PCI. Atherothrombotic burden has been identified as a major determinant of coronary micro-embolization, particularly when plaques are crushed during PCI (31).

Implications and actions needed

Angiography and LBA-determined RSs, obviously, did not enable the optimal stent placement in our study. If the current lesion definition had been used, both methods underestimated PB and lesion length. Clinical benefits of the EBA method extending across the lesion segments seem highly probable (32), but require long-term follow-up validation in a sufficiently large population (33).

Conclusions

The borders of the culprit lesions, according to the current definition (2,3), showed normal vessel structure and acceptable PB infrequently. The lesion boundaries shared similar tissue composition in stable and unstable patients except for higher TCFA accumulation in acute MI. Angiography and LBA-determined RSs did not enable optimal stent placement. Clinical benefits of the EBA method require long-term follow-up validation.

Acknowledgments

Footnote

Reporting Checklist: The authors have completed the STROBE reporting checklist. Available at https://jtd.amegroups.com/article/view/10.21037/jtd-23-924/rc

Data Sharing Statement: Available at https://jtd.amegroups.com/article/view/10.21037/jtd-23-924/dss

Peer Review File: Available at https://jtd.amegroups.com/article/view/10.21037/jtd-23-924/prf

Conflicts of Interest: All authors have completed the ICMJE uniform disclosure form (available at https://jtd.amegroups.com/article/view/10.21037/jtd-23-924/coif). I.D.G. has received grants from Abbott Laboratories, Medtronic Laboratories, and Cryolife Inc. Payments have been provided to the institution in the form of grants and travel support for meetings; none are related to the creation of this manuscript. He is the Program Director for the Brano Heart Failure Forum and has received support related to travel. B.K. has received institutional grants from Saranas, Edwards LifeSciences, LLC, BioVentrix, Inc and Boston Scientific; none are related to the creation of this manuscript. The other authors have no conflicts of interest to declare.

Ethical Statement: The authors are accountable for all aspects of the work in ensuring that questions related to the accuracy or integrity of any part of the work are appropriately investigated and resolved. The study was conducted in accordance with the Declaration of Helsinki (as revised in 2013). The retrospective analysis was approved by the Institutional Review Board of General Hospital Dr. Franc Derganc, Ul. Padlih borcev 13A, 5290 Šempeter pri Gorici (SBG 4/2023). The individual consent was waived because of the retrospective manner of the analysis.

References

1. Davies MJ, Woolf N. Atherosclerosis: what is it and why

does it occur? Br Heart J 1993;69:S3-11.

2. Prati F, Romagnoli E, La Manna A, et al. Long-term consequences of optical coherence tomography findings during percutaneous coronary intervention: the Centro Per La Lotta Contro L'infarto - Optimization Of Percutaneous Coronary Intervention (CLI-OPCI) LATE study. EuroIntervention 2018;14:e443-51.

3. Tearney GJ, Regar E, Akasaka T, et al. Consensus standards for acquisition, measurement, and reporting of intravascular optical coherence tomography studies: a report from the International Working Group for Intravascular Optical Coherence Tomography Standardization and Validation. J Am Coll Cardiol 2012;59:1058-72. Erratum in: J Am Coll Cardiol 2012;59:1662.

4. Mintz GS. Intravascular ultrasound and outcomes after drug-eluting stent implantation. Coron Artery Dis 2017;28:346-52.

5. Mintz GS, Guagliumi G. Intravascular imaging in coronary artery disease. Lancet 2017;390:793-809.

6. Räber L, Mintz GS, Koskinas KC, et al. Clinical use of intracoronary imaging. Part 1: guidance and optimization of coronary interventions. An expert consensus document of the European Association of Percutaneous Cardiovascular Interventions. Eur Heart J 2018;39:3281-300.

7. Morino Y, Tamiya S, Masuda N, et al. Intravascular ultrasound criteria for determination of optimal longitudinal positioning of sirolimus-eluting stents. Circ J 2010;74:1609-16.

8. Wentzel JJ, Gijsen FJH, van der Giessen R, et al. Positive remodeling at 3 year follow up is associated with plaque free coronary wall segment at baseline: A serial IVUS study. Atherosclerosis. 2014;236:82-90.

9. Hoogendoorn A, Gnanadesigan M, Zahnd G, et al. OCT-measured plaque free wall angle is indicative for plaque burden: overcoming the main limitation of OCT? Int J Cardiovasc Imaging 2016;32:1477-81.

10. Thygesen K, Alpert JS, Jaffe AS, et al. Fourth Universal Definition of Myocardial Infarction (2018). J Am Coll Cardiol 2018;72:2231-64.

11. Ryan TJ, Faxon DP, Gunnar RM, et al. Guidelines for percutaneous transluminal coronary angioplasty. A report of the American College of Cardiology/American Heart Association Task Force on Assessment of Diagnostic and Therapeutic Cardiovascular Procedures (Subcommittee on Percutaneous Transluminal Coronary Angioplasty). Circulation 1988;78:486-502.

12. Austen WG, Edwards JE, Frye RL, et al. A reporting

system on patients evaluated for coronary artery disease. Report of the Ad Hoc Committee for Grading of Coronary Artery Disease, Council on Cardiovascular Surgery, American Heart Association. Circulation 1975;51:5-40.

13. The Thrombolysis in Myocardial Infarction (TIMI) trial. Phase I findings. N Engl J Med 1985;312:932-6.

14. Rogers JH, Lasala JM. Coronary artery dissection and perforation complicating percutaneous coronary intervention. J Invasive Cardiol 2004;16:493-9.

15. Otake H, Kubo T, Takahashi H, et al. Optical Frequency Domain Imaging Versus Intravascular Ultrasound in Percutaneous Coronary Intervention (OPINION Trial): Results From the OPINION Imaging Study. JACC Cardiovasc Imaging 2018;11:111-23.

16. Radu MD. The Clinical Atlas of Intravascular Optical Coherence Tomography for iPad. Eur Heart J 2012;33:1174-5.

17. Gonzalo N, Serruys PW, Okamura T, et al. Relation between plaque type and dissections at the edges after stent implantation: an optical coherence tomography study. Int J Cardiol 2011;150:151-5.

18. Kume T, Okura H, Yamada R, et al. Frequency and spatial distribution of thin-cap fibroatheroma assessed by 3-vessel intravascular ultrasound and optical coherence tomography: an ex vivo validation and an initial in vivo feasibility study. Circ J 2009;73:1086-91.

19. Legutko J, Jakala J, Mintz GS, et al. Virtual histology-intravascular ultrasound assessment of lesion coverage after angiographically-guided stent implantation in patients with ST Elevation myocardial infarction undergoing primary percutaneous coronary intervention. Am J Cardiol 2012;109:1405-10.

20. Ali ZA, Maehara A, Généreux P, et al. Optical coherence tomography compared with intravascular ultrasound and with angiography to guide coronary stent implantation (ILUMIEN III: OPTIMIZE PCI): a randomised controlled trial. Lancet 2016;388:2618-28.

21. Dingli P, Gonzalo N, Escaned J. Intravascular Ultrasound-guided Management of Diffuse Stenosis. Radcliffe Cardiology 2018:1-8.

22. Porto I, Di Vito L, Burzotta F, et al. Predictors of periprocedural (type IVa) myocardial infarction, as assessed by frequency-domain optical coherence tomography. Circ Cardiovasc Interv 2012;5:89-96, S1-6.

23. Elakabawi K, Huang X, Shah SA, et al. Predictors of suboptimal coronary blood flow after primary angioplasty and its implications on short-term outcomes in patients with acute anterior STEMI. BMC Cardiovasc Disord

2020;20:391.

24. Kobayashi N, Mintz GS, Witzenbichler B, et al. Prevalence, Features, and Prognostic Importance of Edge Dissection After Drug-Eluting Stent Implantation. An ADAPT-DES Intravascular Ultrasound Substudy. Circ Cardiovasc Interv. 2016;9:e003553.

25. Velican D, Velican C. Comparative study on age-related changes and atherosclerotic involvement of the coronary arteries of male and female subjects up to 40 years of age. Atherosclerosis 1981;38:39-50.

26. Kume T, Akasaka T, Kawamoto T, et al. Assessment of coronary intima--media thickness by optical coherence tomography: comparison with intravascular ultrasound. Circ J 2005;69:903-7.

27. Arnett EN, Isner JM, Redwood DR, et al. Coronary artery narrowing in coronary heart disease: comparison of cineangiographic and necropsy findings. Ann Intern Med 1979;91:350-6.

28. Al-Lamee R, Rajkumar CA, Ganesananthan S, et al. Optimising physiological endpoints of percutaneous coronary intervention. EuroIntervention 2021;16:e1470-83.

29. Virmani R, Burke AP, Kolodgie FD, et al. Pathology of the thin-cap fibroatheroma: a type of vulnerable plaque. J Interv Cardiol 2003;16:267-72.

30. Jang IK, Tearney GJ, MacNeill B, et al. In vivo characterization of coronary atherosclerotic plaque by use of optical coherence tomography. Circulation 2005;111:1551-5.

31. Harrison RW, Aggarwal A, Ou FS, et al. Incidence and outcomes of no-reflow phenomenon during percutaneous coronary intervention among patients with acute myocardial infarction. Am J Cardiol 2013;111:178-84.

32. Prati F, Romagnoli E, Biccirè FG, et al. Clinical outcomes of suboptimal stent deployment as assessed by optical coherence tomography: long-term results of the CLI-OPCI registry. EuroIntervention 2022;18:e150-7.

33. Ali Z, Landmesser U, Karimi Galougahi K, et al. Optical coherence tomography-guided coronary stent implantation compared to angiography: a multicentre randomised trial in PCI - design and rationale of ILUMIEN IV: OPTIMAL PCI. EuroIntervention 2021;16:1092-9.

Appendix 1 Study definitions

Angiographic definitions

Significant coronary lesions

The extent of coronary atherosclerosis was inferred from the distribution of significant coronary obstructions in the major epicardial arteries. A significant lesion was reported as a narrowing of the arterial lumen by ≥50% (34).

Lesion length

Lesion length was measured as a distance between seemingly healthy proximal and distal reference segments. Lesions were graded as discreet (<10 mm), tubular (10–20 mm), or diffuse (>20 mm) (11).

Proximal *vs.* distal lesions

Coronary lesions were located in 15 segments according to the American Heart Association reporting system (12). The lesions originating in the segments 1, 2, 5, 6, 7, 11, and 12 were considered proximal and the remaining distal.

Coronary blood flow

The levels of post-procedural coronary blood flow were assessed by the Thrombolysis in Myocardial Infarction (TIMI) Grade Flow scoring system (13). Grade 0 referred to the absence of any antegrade flow beyond the coronary obstruction; Grade 1 was a faint antegrade flow with incomplete distal filling; Grade 2 was a delayed antegrade flow with complete distal filling; and Grade 3 was the normal antegrade flow.

Edge dissections

Post-procedural edge dissections were categorized according to the National Heart, Lung, and Blood Institute classification system (14). Type A was a minor intra-luminal radiolucent area; Type B was a radiolucent flap that ran parallel with the lumen; in Type C, contrast appeared as a persistent extraluminal flap; in Type D, contrast showed as a persistent spiral filling defect; in Type E, new and persistent defects developed in the vessel lumen; in Type D, all the dissections caused the distal blood flow and progressed to total occlusions.

Optical coherence tomography (OCT) definitions

Normal coronary artery wall

A normal coronary artery wall was defined as a three-layered structure comprising a high back-scattering intima, a low back-scattering media, and a high back-scattering adventitia. The internal elastic membrane (IEM) was defined as the border between the intima and media, and the external elastic membrane (EEM) as the border between the media and adventitia. The maximal intimal thickness was not to exceed 300 µm (3,15,16).

Significant coronary lesions

A coronary lesion was seen as a mass lesion, focal intimal thickening of ≥600 µm, and/or loss of three-layered architecture (3). A significant lesion was defined as a decrease of luminal cross-sectional area by ≥50% compared with the largest reference segment area (3,35).

Proximal reference segments

The proximal reference segment by luminal approach was considered the site with the largest lumen proximal to a stenosis but within the same segment (i.e., usually within 10 mm of the stenosis). This was not necessarily the site with the least plaque (3,35). The proximal segment by the EEM approach was considered the site proximal to a stenosis with ≥180° of EEM visible (20).

Distal reference segments

The distal reference segment by luminal approach was considered the site with the largest lumen distal to a stenosis but within

https://dx.doi.org/10.21037/jtd-23-924

the same segment (i.e., usually within 10 mm of the stenosis). This was not necessarily the site with the least plaque (3,35). The distal reference segment by EEM approach was considered the site distal to a stenosis with ≥180° of EEM visible (20).

Lesion border detection
An acceptable OCT visibility was deemed if ≥50% (≥180°) of the reference segment circumference was detected (15,36).

Lesion length
By luminal-based approach (LBA), lesion length was the distance from proximal to distal reference sites using the OCT automated lumen detection feature. By EEM-based approach (EBA), lesion length was determined as the distance from proximal to distal reference site when the border visibility was acceptable (≥180°) (20).

Atherosclerotic plaque types
Atherosclerotic plaques were classified as fibrous plaques, fibro-calcific plaques, and fibroatheromas. All diagnoses were made at the cross-sectional level, and the dominant type provided the basis for the classification (16).

Fibrous plaques
A fibrous plaque was defined as a high backscattering and relatively homogeneous intimal thickening of ≥600 µm with lipid pools or calcifications involving <1 quadrant in the cross-section (3,16).

Fibro-calcific plaques
A fibrocalcific plaque was characterized by the evidence of sharply delineated signal-poor calcifications, embedded in signal-rich fibrous tissue and extending > 1 quadrant in the cross-section (3,16).

Fibroatheromas
A fibroatheroma was defined as a lesion with an OCT-delineated fibrous cap and a necrotic core. The necrotic core was seen as a diffusely demarcated signal-poor region with high light attenuation and involving >1 quadrant in the cross-section (3,16). A thick-capped fibroatheroma (ThCFA) was defined as a fibroatheroma with a delineated necrotic core and an overlying fibrous cap with a thickness of ≥65 µm (3). A thin-capped fibroatheroma (TCFA) was defined as a lipid-rich plaque with a fibrous cap thickness of <65 µm and a maximum lipid arc >90° (35).

Ruptured plaques
A ruptured plaque was a fibroatheroma that showed features of intimal tearing, disruption, or dissection of the cap and a cavity formation inside the plaque (3).

Plaque erosions
Plaque erosion was composed of OCT evidence of thrombus, irregular luminal surface, and no evidence of cap rupture evaluated in multiple adjacent frames (3).

Thrombi
A thrombus was a mass attached to the luminal surface or floating within the lumen. Red thrombus was highly backscattering and had a high signal attenuation, while white thrombus was less backscattering, homogeneous, and had low signal attenuation (3).

Plaque burden
The EEM, visible for ≥220° of the vessel wall circumference, was a surrogate marker for plaque burden <40% (9).

Stent edges
Stent edge was defined as the first or last cross-section exhibiting visible struts in a circumference of <360°. The first and

last cross-sections with visible struts in a circumference of 360° were defined as the stented segment. Cross sections 5-mm proximal or distal to stent edges were considered as the marginal segments (37).

Edge dissections

An edge dissection was defined as a disruption of the luminal vessel surface in the edge segments within 5 mm proximal and distal to the stent. Major edge dissections were considered dissections with ≥60° of the circumference of the vessel at the site of dissection and/or ≥3 mm in length. Smaller injuries were judged as minor dissections (16).

References

34. Comparison of coronary bypass surgery with angioplasty in patients with multivessel disease. N Engl J Med 1996;335:217-25.
35. Prati F, Regar E, Mintz GS, et al. Expert review document on methodology, terminology, and clinical applications of optical coherence tomography: physical principles, methodology of image acquisition, and clinical application for assessment of coronary arteries and atherosclerosis. Eur Heart J 2010;31:401-15.
36. OPtical Coherence Tomography (OCT) Guided Coronary Stent IMplantation Compared to Angiography: a Multicenter Randomized TriaL in PCI. ILUMIEN-IV. NCT03507777. July 22, 2019.
37. Gogas BD, Garcia-Garcia HM, Onuma Y, et al. Edge vascular response after percutaneous coronary intervention: an intracoronary ultrasound and optical coherence tomography appraisal: from radioactive platforms to first- and second-generation drug-eluting stents and bioresorbable scaffolds. JACC Cardiovasc Interv 2013;6:211-21.
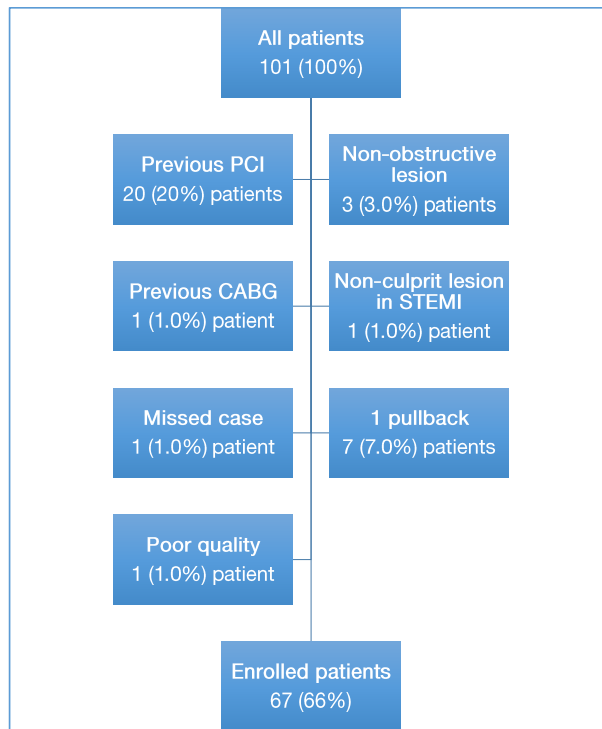
Figure S1 Flow chart of the patient enrollment in the study. Out of 101 patients planned for single culprit vessel PCI having OCT imaging, 67 (66%) patients were enrolled in the study. The entry criteria were: single-vessel culprit lesion PCI, baseline and post-stenting OCT pullbacks, no previous PCI/CABG of the culprit vessel, and adequate imaging quality. PCI, percutaneous coronary intervention; CABG, coronary artery bypass graft; STEMI, ST-segment elevation myocardial infarction; OCT, optical coherence tomography.

Table S1 Visibility of external elastic membrane in reference and adjacent marginal segments

Variable	All patients (n=67)	Group 1 (n=34)	Group 2 (n=33)	P value
Proximal RS, n (%)				
≥220°	19 (28.4)	7 (20.6)	12 (36.4)	0.152
≥180°	45 (67.2)	24 (70.6)	21 (63.6)	0.545
<180°	22 (32.8)	10 (29.4)	12 (36.4)	0.545
Proximal AMS 1, n (%)				
≥220°	20 (29.9)	10 (29.4)	10 (30.3)	0.936
≥180°	44 (65.7)	24 (70.6)	20 (60.6)	0.390
<180°	23 (34.3)	10 (29.4)	13 (39.4)	0.390
Proximal AMS 2, n (%)				
≥220°	14 (20.9)	8 (23.5)	6 (18.2)	0.590
≥180°	45 (67.2)	26 (76.5)	19 (57.5)	0.100
<180°	22 (32.8)	8 (23.5)	14 (42.4)	0.100
Proximal AMS 3, n (%)				
≥220°	14 (20.9)	5 (14.7)	9 (27.2)	0.206
≥180°	33 (49.3)	25 (73.5)	13 (39.4)	0.112
<180°	34 (50.7)	14 (41.2)	20 (58.8)	0.112
Proximal AMS 4, n (%)				
≥220°	12 (17.9)	4 (11.8)	8 (24.2)	0.507
≥180°	34 (50.7)	18 (52.9)	16 (48.5)	0.715
<180°	33 (49.3)	16 (47.0)	17 (51.6)	0.544
Proximal AMS 5, n (%)				
≥220°	13 (19.4)	6 (17.7)	7 (21.2)	0.712
≥180°	34 (50.7)	19 (55.9)	15 (45.4)	0.273
<180°	33 (49.3)	15 (44.1)	18 54.6)	0.273
Distal RS, n (%)				
≥220°	21 (31.3)	12 (35.3)	9 (27.2)	0.479
≥180°	37 (55.2)	18 (52.9)	19 (57.6)	0.703
<180°	30 (44.8)	16 (47.0)	14 (42.4)	0.703
Distal AMS 1, n (%)				
≥220°	22 (32.8)	12 (35.3)	10 (30.3)	0.664
≥180°	42 (62.7)	23 (67.6)	19 (57.6)	0.271
<180°	25 (37.3)	11 (32.3)	14 (42.4)	0.394
Distal AMS 2, n (%)				
≥220°	25 (37.3)	13 (38.2)	12 (36.4)	0.882
≥180°	42 (62.7)	23 (67.6)	19 (57.6)	0.394
<180°	25 (37.3)	11 (32.3)	14 (42.4)	0.394
Distal AMS 3, n (%)				
≥220°	24 (35.8)	12 (35.3)	12 (36.4)	0.927
≥180°	44 (65.7)	23 (67.6)	21 (63.6)	0.730
<180°	23 (34.3)	11 (32.3)	12 (36.4)	0.730
Distal AMS 4, n (%)				
≥220°	26 (38.8)	12 (35.3)	14 (42.4)	0.549
≥180°	48 (71.6)	23 (67.6)	25 (75.7)	0.462
<180°	19 (28.4)	11 (32.3)	8 (27.2)	0.462
Distal AMS 5, n (%)				
≥220°	28 (41.8)	12 (35.3)	16 (48.4)	0.274
≥180°	49 (73.1)	22 (64.7)	27 (81.8)	0.114
<180°	18 (26.9)	12 (35.3)	6 (18.2)	0.114

Groups 1 and 2 are compared using χ^2 test. Group 1, patients with acute myocardial infarction; Group 2, patients with stable coronary artery disease. RS, reference segment; AMS 1 – 5, adjacent marginal segment 1 mm to 5 mm beyond the RS.

Table S2 Qualitative optical coherence tomography characteristics

Variable	All patients (n=67)	Group 1 (n=34)	Group 2 (n=33)	P value
Proximal RS, n (%)				0.539
N	6 (9.0)	2 (5.8)	4 (12.1)	
FP	33 (49.3)	18 (52.9)	15 (45.4)	
ThCFA	7 (10.4)	4 (12.1)	3 (9.1)	
TCFA	2 (3.0)	2 (5.8)	0 (0)	
FCP	19 (28.3)	8 (23.5)	11 (33.3)	
Minimal area, n (%)				<0.001
N	0 (0)	0 (0)	0 (0)	
FP	12 (17.9)	2 (5.9)	10 (30.3)	
ThCFA	11 (16.4)	3 (8.8)	8 (24.3)	
TCFA	24 (35.8)	23 (67.6)	1 (3.0)	
FCP	17 (25.4)	4 (11.8)	13 (39.4)	
Calc Nod	3 (4.5)	2 (5.9)	1 (3.0)	
Distal RS, n (%)				0.608
N	9 (13.5)	5 (14.7)	4 (12.1)	
FP	29 (43.3)	16 (47.2)	13 (39.4)	
ThCFA	8 (11.9)	3 (8.8)	5 (15.2)	
TCFA	2 (3.0)	2 5.8)	0 (0)	
FCP	19 (28.3)	8 (23.5)	11 (33.3)	

Groups 1 and 2 are compared using χ^2 test. Group 1, patients with acute myocardial infarction; Group 2, patients with stable coronary artery disease. RS, reference segment; N, normal vessel wall; FP, fibrous plaque; ThCFA, thick-cap fibroatheroma; TCFA, thin-cap fibroatheroma; FCP, fibrocalcific plaque; Calc Nod, calcified nodule.

Table S3 Plaques in adjacent marginal segments 1 (i.e., 1 mm beyond the reference segment)

Variable	All patients (n=67)	Group 1 (n=34)	Group 2 (n=33)	P value
Prox AMS, n (%)				0.269
N	6 (9.0)	2 (5.9)	4 (12.1)	
FP	27 (40.3)	16 (47.1)	11 (33.3)	
ThCFA	14 (20.9)	8 (23.5)	6 (18.2)	
TCFA	2 (2.9)	2 (5.9)	0 (0)	
FCP	18 (26.9)	6 (17.6)	12 (36.4)	
Dist AMS, n (%)				0.817
N	9 (13.5)	6 (17.7)	3 (9.1)	
FP	30 (44.8)	15 (44.1)	15 (45.5)	
ThCFA	7 (10.4)	4 (11.8)	3 (9.1)	
TCFA	0 (0)	0 (0)	0 (0)	
FCP	21 (31.3)	9 (26.5)	12 (36.4)	

Groups 1 and 2 are compared using χ^2 test. Group 1, patients with acute myocardial infarction; Group 2, patients with stable coronary artery disease. Prox AMS 1, proximal adjoining marginal segment 1 mm beyond the reference segment; Dist AMS, distal adjacent marginal segment; N, normal; FP, fibrous plaque; ThCFA, thick-cap fibroatheroma; TCFA, thin-cap fibroatheroma; FCP, fibrocalcific plaque.

Table S4 Plaques in adjacent marginal segments 2 (i.e., 2 mm beyond the reference segment)

Variable	All patients (n=67)	Group 1 (n=34)	Group 2 (n=33)	P value
Prox AMS 2, n (%)				0.295
N	6 (9.0)	2 (5.9)	4 (12.1)	
FP	24 (35.8)	14 (41.2)	10 (30.3)	
ThCFA	13 (19.4)	7 (20.6)	6 (18.2)	
TCFA	3 (4.5)	3 (8.8)	0 (0)	
FCP	21 (31.3)	8 (23.5)	13 (39.4)	
Dist AMS 2, n (%)				0.319
N	9 (13.5)	6 (17.7)	3 (9.1)	
FP	26 (38.8)	15 (44.1)	11 (33.3)	
ThCFA	7 (10.4)	3 (8.8)	4 (12.1)	
TCFA	2 (3.0)	2 (5.9)	0 (0)	
FCP	23 (34.3)	8 (23.5)	15 (45.5)	

Groups 1 and 2 are compared using χ^2 test. Group 1, patients with acute myocardial infarction; Group 2, patients with stable coronary artery disease. Prox AMS, proximal adjacent marginal segment; Dist AMS, distal adjacent marginal segment; N, normal; FP, fibrous plaque; ThCFA, thick-cap fibroatheroma; TCFA, thin-cap fibroatheroma; FCP, fibrocalcific plaque.

Table S5 Plaques in adjacent marginal segments 3 (i.e., 3 mm beyond the reference segment)

Variable	All patients (n=67)	Group 1 (n=34)	Group 2 (n=33)	P-value
Prox AMS 3, n (%)				.434
N	7 (10.5)	3 (8.8)	4 (12.1)	
FP	23 (34.3)	13 (38.2)	10 (30.3)	
ThCFA	14 (20.9)	8 (23.5)	6 (18.2)	
TCFA	2 (3.0)	2 (5.9)	0 (0)	
FCP	21 (31.3)	8 (23.5)	13 (39.4)	
Dist AMS 3, n (%)				.946
N	9 (13.5)	6 (17.7)	3 (8.8)	
FP	26 (38.8)	13 (38.2)	13 (38.2)	
ThCFA	10 (14.9)	5 (14.7)	5 (14.7)	
TCFA	2 (3.0)	1 (2.9)	1 (2.9)	
FCP	20 (29.9)	9 (26.5)	11 (37.4)	

Groups 1 and 2 are compared using χ^2 test. Group 1, patients with acute myocardial infarction; Group 2, patients with stable coronary artery disease. Prox AMS, proximal adjacent marginal segment; Dist AMS, distal adjacent marginal segment; N, normal; FP, fibrous plaque; ThCFA, thick-cap fibroatheroma; TCFA, thin-cap fibroatheroma; FCP, fibrocalcific plaque.

Table S6 Plaques in adjacent marginal segments 4 (i.e., 4 mm beyond the reference segment)

Variable	All patients (n=67)	Group 1 (n=34)	Group 2 (n=33)	P value
Prox AMS 4, n (%)				0.291
N	7 (10.5)	3 (8.8)	4 (12.1)	
FP	26 (38.8)	15 (44.1)	11 (32.3)	
ThCFA	10 (14.9)	6 (17.6)	4 (12.1)	
TCFA	3 (4.5)	3 (8.8)	0 (0)	
FCP	21 (31.3)	7 (20.6)	14 (42.4)	
Dist AMS 4, n (%)				0.919
N	9 (13.5)	6 (17.7)	3 (9.1)	
FP	27 (40.3)	14 (41.2)	13 (39.4)	
ThCFA	8 (11.9)	4 (11.8)	4 (12.1)	
TCFA	2 (3.0)	1 (2.9)	1 (3.0)	
FCP	21 (31.3)	9 (26.5)	12 (36.4)	

Groups 1 and 2 are compared using χ^2 test. Group 1, patients with acute myocardial infarction; Group 2, patients with stable coronary artery disease. Prox AMS, proximal adjacent marginal segment; Dist AMS, distal adjacent marginal segment; N, normal; FP, fibrous plaque; ThCFA, thick-cap fibroatheroma; TCFA, thin-cap fibroatheroma; FCP, fibrocalcific plaque.

Table S7 Plaques in adjacent marginal segments 5 (i.e., 5 mm beyond the reference segment)

Variable	All patients (n=67)	Group 1 (n=34)	Group 2 (n=33)	P-value
Prox AMS 5, n (%)				.336
N	6 (9.0)	2 (5.9)	4 (12.1)	
FP	26 (38.8)	15 (44.1)	11 (33.3)	
ThCFA	10 (14.9)	6 (17.6)	4 (12.1)	
TCFA	3 (4.5)	3 (8.8)	0 (0)	
FCP	22 (32.8)	8 (23.5)	14 (42.4)	
Dist AMS 5, n (%)				.752
N	9 (13.5)	6 (17.7)	3 (9.1)	
FP	25 (37.3)	13 (38.2)	12 (36.4)	
ThCFA	9 (13.4)	5 (14.7)	4 (12.1)	
TCFA	2 (3.0)	1 (8.8)	1 (3.0)	
FCP	22 (32.8)	9 (26.5)	13 (39.4)	

Groups 1 and 2 are compared using χ^2 test. Group 1, patients with acute myocardial infarction; Group 2, patients with stable coronary artery disease. Prox AMS, proximal adjacent marginal segment; Dist AMS, distal adjacent marginal segment; N, normal; FP, fibrous plaque; ThCFA, thick-cap fibro-atheroma; TCFA, thin-cap fibro-atheroma; FCP, fibrocalcific plaque.

Table S8 Predictors of periprocedural complications according to regression analysis

Variable	Univariate analysis			Multivariate analysis		
	OR	95% CI	P value	OR	95% CI	P value
Thrombolysis in myocardial infarction flow ≤3						
Hypertension, +	14.3	1.46–140.5	0.022			
STEMI, −	0.049	0.005–0.49	0.01	0.032	0.002–0.825	0.037
Patent culprit, +	0.130	0.02–0.87	0.038			
TCFA at RSs, −	0.087	0.01–0.073	0.025			
TCFA at prox. RSs, −	0.028	0.002–0.4	0.008			
Edge dissection						
Gender, male	3.37	1.09–10.38	0.035			
Hypertension, +	3.8	2.0–12.09	0.024			
Previous angina, +	5	1.28–19.53	0.021			
AMI, +	3.34	1.03–10.86	0.045			
STEMI, −	0.15	0.39–0.54	0.004			
Aspirin, previous	4.6	1.18–17.97	0.028			
Stent diameter, mm	3.98	1.12–14.11	0.032			

OR, odds ratio; CI, confidence interval; +, variable present; −, variable absent; STEMI, ST-elevation myocardial infarction; TCFA, thin-cap fibroatheroma; RSs, reference segments; prox, proximal; AMI, acute myocardial infarction.